The Advantages of Being Locked

ASSESSING THE CLEAVAGE OF SHORT AND LONG RNAs BY LOCKED NUCLEIC ACID-CONTAINING 8–17 DEOXYRIBOZYMES*[S]

Stefano Donini[‡1], **Marcello Clerici**[‡], **Jesper Wengel**[§], **Birte Vester**[¶2], and **Alessio Peracchi**[‡3]

From the ‡Department of Biochemistry and Molecular Biology, University of Parma, 43100 Parma, Italy, ¶Nucleic Acid Center, Department of Biochemistry and Molecular Biology, University of Southern Denmark, DK-5230 Odense M, Denmark, and §Nucleic Acid Center, Department of Chemistry, University of Southern Denmark, DK-5230 Odense M, Denmark

RNA-cleaving deoxyribozymes can be used for the sequence-specific knockdown of mRNAs. It was previously shown that activity of these deoxyribozymes is enhanced when their substrate-binding arms include some locked nucleic acid (LNA) residues, but the mechanistic basis of this enhancement was not explored. Here we dissected the kinetics and thermodynamics underlying the reaction of LNA-containing 8–17 deoxyribozymes. Four 8–17 constructs were designed to target sequences within the E6 mRNA from human papillomavirus type 16. When one of these deoxyribozymes (DNAzymes) and the corresponding LNA-armed enzyme (LNAzyme) were tested against a minimal RNA substrate, they showed similar rates of substrate binding and similar rates of intramolecular cleavage, but the LNAzyme released its substrate more slowly. The superior thermodynamic stability of the LNAzyme-substrate complex led to improved performances in reactions carried out at low catalyst concentrations. The four DNAzymes and the corresponding LNAzymes were then tested against extended E6 transcripts (>500 nucleotides long). With these structured substrates, the LNAzymes retained full activity, whereas the DNAzymes cleaved extremely poorly, unless they were allowed to pre-anneal to their targets. These results imply that LNAzymes can easily overcome the kinetic barrier represented by local RNA structure and bind to folded targets with a faster association rate as compared with DNAzymes. Such faster annealing to structured targets can be explained by a model whereby LNA monomers favor the initial hybridization to short stretches of unpaired residues ("nucleation"), which precedes disruption of the local mRNA structure and completion of the binding process.

In the past decade, several RNA-cleaving deoxyribozymes (DNAzymes)[4] have been isolated in the laboratory through the application of a combinatorial technique known as "*in vitro* selection" (1). The two most prominent examples are the 8–17 and 10–23 deoxyribozymes, originally identified in the Joyce laboratory (2). Both types of deoxyribozymes comprise a central "core" and two substrate-binding arms that can be varied in length and sequence. The chemical stability of these catalysts, their ease of synthesis, and versatility in the sequence-specific cleavage of RNA have prompted a wealth of studies on the potential use of DNAzymes in therapy, to inhibit the expression of disease-causing genes by selectively binding and cleaving the corresponding mRNAs (*e.g.* (3–5)).

However, several factors limit the practical use of DNAzymes as anti-gene agents. For example, it may be difficult to achieve an intercellular concentration of DNAzyme high enough to ensure stable binding to the target mRNA and hence efficient knockdown. In part, this problem can be countered by lengthening the substrate-recognition arms, thus increasing the affinity of the DNAzyme for its target, but this entails the synthesis of larger DNA molecules, which are less manageable and more prone to the adoption of alternative structures and to off-target binding. The binding problem is made even worse by the potentially limited accessibility of the intended target sequence within the mRNA structure. Indeed, there are suggestions that up to 90% of potential cleavage sites in long mRNAs are inaccessible to classical DNAzymes (6, 7) presumably because of a complex secondary and tertiary folding of these RNAs.

An important step forward in solving these problems of efficient binding at low DNAzyme concentrations and of target accessibility has been the introduction of LNA (Fig. 1*A*). LNA residues are capable of normal Watson-Crick base pairing, and the locked sugar enhances the preorganization of the phosphate backbone, stabilizing the helical (A-type) structure of a duplex (8–10). Several studies have shown that the inclusion of a few LNA monomers into the arms of the 10–23 deoxyribozyme significantly improves the performances of this catalyst against small RNA substrates and, more pronouncedly, against

---

[4] The abbreviations used are: DNAzyme, a deoxyribozyme construct composed entirely of DNA; LNA, locked nucleic acid; LNAzyme, LNA-armed enzyme; LNAzyme, a deoxyribozyme construct containing some LNA nucleotides in the substrate-binding arms; HPV16, human papillomavirus type 16; PIPES, 1,4-piperazinediethanesulfonic acid; nt, nucleotide; HPV16, human papillomavirus type 16.
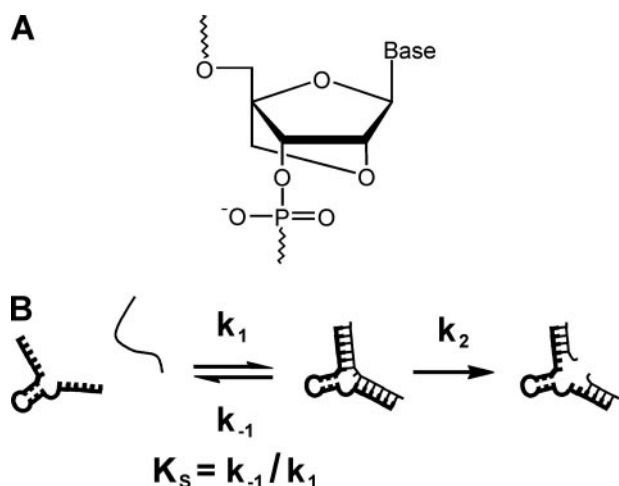
FIGURE 1. *A,* structure of an LNA nucleotide. *B,* minimal kinetic scheme for the RNA cleavage reaction carried out by a DNAzyme (or LNAzyme) under single-turnover conditions. The catalyst (drawn with a *dark line*) must bind its substrate (*thin line*) to form a productive bimolecular complex. Within this complex, the target RNA is cleaved to yield two products, one of which containing a cyclic 2′,3′-phosphate (2).

long RNA transcripts, promoting cleavage of highly structured RNAs (11–17).

Although LNA monomers are expected to increase the affinity of a deoxyribozyme for its target, the kinetics and thermodynamics underlying the observed catalytic enhancements have not been analyzed in detail. With respect to a minimal kinetic scheme for a deoxyribozyme reaction (Fig. 1*B*), it remains to be established whether the increased affinity alone can explain the improved kinetics, or if LNA also accelerates the intramolecular cleavage step (described by the kinetic constant k_2) (11, 16). Furthermore, the LNA monomers could in principle improve the RNA binding affinity of deoxyribozymes via an increased association rate (k_1) or a reduced dissociation rate (k_{-1}), or both; data from model systems are somewhat contradictory on this point (18, 19). Finally, it is not completely obvious why the improved performances of LNA-containing deoxyribozymes were particularly evident against long RNA transcripts.

In relation to these issues, we provide here a detailed kinetic comparison between a well characterized 8–17 construct and a corresponding LNA-armed version. Furthermore, we contrast the performances of four DNAzyme/LNAzyme pairs targeted against different regions of a viral RNA transcript (the E6 mRNA from HPV16). Our findings indicate the following. (i) LNA monomers located in the deoxyribozyme arms have only minimal effects on the cleavage step (k_2). (ii) LNA monomers greatly reduce the rate of substrate dissociation (k_{-1}), stabilizing the catalyst-substrate complex. (iii) Finally, the effect on the association step (k_1) depends on the type of substrate; with short, unstructured substrates, k_1 is nearly equal for DNAzymes and LNAzymes, whereas with long, structured RNAs, the association is substantially faster for LNAzymes as compared with DNAzymes.

EXPERIMENTAL PROCEDURES

Oligonucleotides—DNA oligonucleotides were from MWG Biotec (Ebersberg, Germany) or from DNATechnology (Aar-

hus, Denmark). LNAzymes were synthesized using published procedures (20). The minimal (17-mer) RNA substrate for Dz122 and Lz122 was from Dharmacon Research (Lafayette, CO), and when necessary it was ^{32}P-5′-end-labeled with T4 polynucleotide kinase. The other minimal substrates were synthesized with T7 RNA polymerase (Promega), employing the following templates: S32 template, 5′-GTGGTAACTTTCTGGGT-CCTATAGTGAGTCGTATTAG-3′; S51 template, 5′-TGCAG-CTCTGTGCATAACCTATAGTGAGTCGTATTAG-3′; S122 template, 5′-CATATACCTCACGTCGCCCTATAGTGAGTC-GTATTAG-3′; 163 template, 5′-CCCATCTCTATATA-CTACCTATAGTGAGTCGTATTAG-3′.

The templates were hybridized to the complementary deoxyoligonucleotide 5′-TAATACGACTCACTATAGG-3′ to form a double-stranded T7 promoter. Transcription was conducted using the buffer conditions recommended by the supplier and 1 mM nucleoside triphosphates. After transcription, the reaction mixtures were extracted and precipitated, and the full-length RNAs were isolated on a 7 M urea, 13% polyacrylamide gel. RNAs were eluted from gel bands, extracted with phenol/chloroform, ethanol-precipitated, and redissolved in H$_2$O. RNA transcripts were generally 5′-radiolabeled by dephosphorylating using shrimp phosphatase (U. S. Biochemical Corp.) and subsequently incubating with T4 polynucleotide kinase (New England Biolabs) and [γ-^{32}P]ATP. Concentrations of radioactive oligonucleotides were determined from specific activities; concentrations of nonradioactive oligonucleotides were determined using extinction coefficients at 260 nm estimated by the nearest neighbor method (21).

In Vitro Transcription of E6 and E6E7 mRNA—The E6 and E6E7 mRNAs from HPV16 were transcribed *in vitro* from the corresponding genes. Two plasmids containing the E6 coding sequence (BSK-16-E6) and the E6E7 coding sequence (BKS-16-E6E7) were kindly provided by Massimo Tommasino (International Agency for Research on Cancer, Lyon, France). These were Bluescript plasmids (the complete sequence and list of restriction sites are available on line; GenBank^{TM} accession number X52327 (K_S(+)) and 52328 (SK(+)).

The plasmids were first cut with XhoI (a restriction enzyme whose cleavage site is located in both constructs, shortly downstream of the stop codon, see supplemental Fig. 1) and then transcribed using either T3 RNA polymerase (for E6 RNA) or T7 RNA polymerase (for the E6E7 RNA). The transcription mixture (50 μl) for the nonradioactive substrates contained the following: 10 μl of 5× transcription buffer, 7 mM nucleoside triphosphate, 26 mM MgCl$_2$, 30 mM dithiothreitol, 750 ng of template, and 17 units of T3 RNA polymerase (Amersham Biosciences), or 20 units of T7 RNA polymerase (Stratagene). The transcription mixture (20 μl) for the radioactive substrate contained: 4 μl of 5× transcription buffer, 1 mM nucleoside triphosphate, 10 mM MgCl$_2$, 10 mM dithiothreitol, 29 units of RNasin, 2 μg of template, and polymerases as above.

After transcription, the RNAs were extracted with phenol/chloroform, precipitated, and purified on a 7 M urea, 6% polyacrylamide gel. Full-length transcripts were eluted from gel bands using 2 M NH$_4$Ac, pH 5.3 (elution overnight with 150 μl and wash with 100 μl), extracted with phenol/chloroform, ethanol-precipitated, and redissolved in H$_2$O. Concentrations of

radioactive and nonradioactive oligonucleotides were determined using extinction coefficients at 260 nm estimated by the nearest neighbor method (21).

Measurement of Individual Rate Constants for Dz122 and Lz122—Reactions of Dz122 and Lz122 against a minimal substrate (17-nt long) were conducted in 50 mM PIPES-NaOH, pH 7.4, 3 mM Mg^{2+}, to allow a direct comparison with an earlier study (22) where the Dz122 construct was characterized in detail.

Cleavage reactions were single turnover, with the catalyst in large excess ($\geq$10-fold) with respect to the labeled substrate, so that the product dissociation step did not affect the observed kinetics (22). Substrate and catalyst were separately heated at 95 °C for 2 min to disrupt potential aggregates, spun briefly in a microcentrifuge, and equilibrated for 10–30 min at the reaction temperature. After supplementing the catalyst tube with $MgCl_2$, reactions were initiated by adding the substrate. Time points were collected at appropriate intervals, and further reaction was quenched by adding formamide and excess EDTA. Radiolabeled substrates and products were separated on 7 M urea, 20% polyacrylamide gels and quantitated by PhosphorImaging. Reaction time courses were fit to the appropriate kinetic equation using SigmaPlot (SPSS Inc.).

k_2 (describing cleavage within the enzyme-substrate complex) was measured by employing saturating concentrations of the catalyst ($\geq$1 μM) to ensure that all the substrates would be bound to the DNAzyme or LNAzyme (22). As a control that saturation of the substrate was achieved, the measured rate constants remained identical, within error, when the concentration of catalyst was raised from 1 μM to 5 or 10 μM.

The rate constants for substrate dissociation (k_{-1}) and association (k_1) were measured through a pulse-chase strategy (22). To determine k_{-1}, a saturating concentration of DNAzyme or LNAzyme (100 nM) was first allowed to bind a trace amount of radiolabeled substrate ($\sim$0.1 nM) for 4 min, in the presence of 3 mM $MgCl_2$ (over this time, <1% of the substrate was cleaved). Then a large excess of unlabeled substrate (1 μM final) was added to initiate the "chase" period, during which dissociation of labeled substrate from the catalyst was essentially irreversible. An otherwise identical reaction, but without the chase, was carried out in parallel. Partitioning of the labeled substrate between cleavage and release depended on the relative magnitude of k_{-1} and k_2. In particular, the fractional extent of cleavage in the presence of the chase (relative to the extent in the absence of chase) reflected the ratio $k_2/(k_{-1} + k_2)$ (23). Thus, measuring k_2 and the final extent of cleavage allowed determination of k_{-1}.

A pulse-chase method was also used to determine k_1. In these experiments, an excess DNAzyme or LNAzyme (1–15 nM) was first allowed to bind a trace amount of radiolabeled substrate for a period, t_1, variable from 0.5 to 7 min (over this time, <1% of the substrate was cleaved). Then the sample was transferred into a solution containing a large excess of unlabeled substrate (to prevent any further binding of radioactive substrate) as well as 15 mM Mn^{2+}, pH 7.8. Because of the high concentration of Mn^{2+} and the increased pH, all the bound labeled substrate was cleaved in less than 3 min (22), so that the fraction of cleaved substrate reflected the amount of catalyst-substrate complex

formed at t_1. The dependence of such a fraction on t_1 was fit to a single exponential function, yielding a pseudo-first order rate constant for substrate binding, k_{app}. k_1 was obtained from a linear regression of the k_{app} values *versus* the catalyst concentration.

Cleavage of Long RNA Transcripts—Cleavage of the E6 and E6E7 mRNAs were measured under single-turnover conditions at 37 °C. The reaction buffer contained 50 mM Tris-HCl, pH 7.5, 150 mM NaCl, and 0.008% SDS.

Two distinct kinetic protocols were used. In protocol A, the DNAzyme (or LNAzyme) and the mRNA substrate were heated separately in reaction buffer, in the presence of 10 mM $MgCl_2$. After this heating step (2 min at 80 °C), the samples were spun briefly in a microcentrifuge and equilibrated for 10 min at the reaction temperature. The cleavage reactions were initiated by mixing the catalyst and substrate solutions. The reaction mixture contained 10 nM RNA (final concentration) and 100 nM catalyst (10-fold molar excess). Aliquots were collected at appropriate times and quenched by adding formamide and excess EDTA.

In protocol B, cleavage rates were determined after pre-annealing the catalyst and the mRNA. Annealing was achieved by heating together the DNAzyme (or LNAzyme) and RNA in reaction buffer at 80 °C for 2 min, followed by cooling in two steps (50 °C for 5 min; 37 °C for 10 min). The cleavage reactions were then started by adding $MgCl_2$ to a final concentration of 10 mM. The concentrations of enzyme and RNA were as above.

Substrates and products of the cleavage reactions were separated on 6% polyacrylamide gels and quantitated by a PhosphorImager. The fraction of product at time t, F_t, was calculated by dividing the amount of product by the amount of substrate plus product, and the data were fit to a single-exponential function as shown in Equation 1,

$$F_t = F_\infty(1 - e^{-k_{obs}t})$$ (Eq. 1)

where F_∞ is the fraction of product at the end point of the reaction, and k_{obs} is the rate constant of cleavage (23). Sometimes the reaction was clearly biphasic, and the data were hence fit to a double exponential function as shown in Equation 2,

$$F_t = F_1(1 - e^{-k_{obs1}t}) + F_2(1 - e^{-k_{obs2}t})$$ (Eq. 2)

where F_1 and F_2 represent the end points of the first and second phase of the time course, respectively.

RESULTS

Constructs Used—In this study, we compared the activities of four conventional 8–17 DNAzymes with their partially LNA-armed counterparts (LNAzymes; Fig. 2). All four 8–17 constructs were directed against the E6 mRNA from HPV16. This mRNA is a well established model system to explore the application of antisense and catalytic antisense oligonucleotides, and much experimental information is available about the accessibility of different parts of the RNA sequence (*e.g.* see Refs. 6, 24–26).

The four 8–17 constructs were designed to cleave at specific AG sites, located within the first 200 nucleotides of the E6 coding sequence. Dz32 was designed to hybridize to a sequence
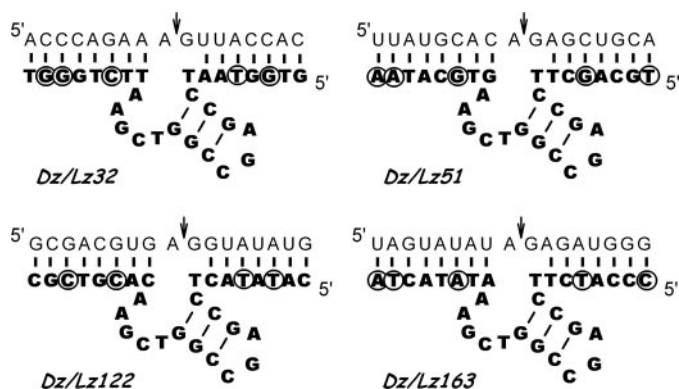
FIGURE 2. **Primary and secondary structures of the 8–17 DNAzymes and LNAzymes used in this study.** The four constructs were designed to recognize 17-nt-long RNA targets on the E6 RNA. The number in the name of each construct refers to the position of cleavage within the E6 coding sequence. Against each target we tested one 8–17 DNAzyme (composed only of DNA monomers) and one LNAzyme (in which four or five nucleotides in the arms were replaced by LNA monomers). DNA is shown in *boldface letters,* and the positions at which LNA monomers were introduced are *circled*. Note that cytidine LNA residues are methylated at the 5-position. The RNA target sequences are shown as *normal letters,* and the *arrows* indicate the cleavage sites.

TABLE 1

Comparison of the catalytic parameters for the reactions catalyzed by Dz122 and Lz122

Conditions are as follows: PIPES-NaOH buffer, pH 7.4, 3 mM Mg^{2+}. Data are the average of at least two independent determinations, which differed by less than 25% from each other. The k_1 and k_{-1} values for the Dz122 construct had already been reported in Ref. 22.

Construct	Temperature	k_2	k_1	k_{-1}	K_S
	°C	*min^{-1}*	*$M^{-1}min^{-1}$*	*min^{-1}*	*nM*
Dz122	25	10^{-2}	1.7×10^7	2×10^{-2}	1.2
Lz122	25	6×10^{-3}	3.3×10^7	1.6×10^{-3}	0.05
Dz122	37	2.8×10^{-2}			
Lz122	37	2.2×10^{-2}			

that overlaps the best target sequence identified by Pan *et al.* (25), who tested the accessibility of the E6 mRNA by using a library of hammerhead ribozymes. The Dz122 target sequence includes two of the four best cleavage sites identified by Cairns *et al.* (6), using a library of 10–23 deoxyribozymes. The target of Dz163 encompassed one accessible cleavage site identified by Pan *et al.* (25) and two accessible sites described by Cairns *et al.* (6). Finally, Dz51 was used as a control; it targets a sequence that previous studies found only modestly accessible (6, 25), but RNA folding software such as mFold (27) predicted that the cleavage site would lie in a single-stranded region.

Kinetic and Thermodynamic Comparison of Dz122 and Lz122—The construct Dz122 had been kinetically well characterized in previous studies, where it was named (8–17)*cb* (22, 28, 29). Therefore, we employed this construct for a detailed kinetic and thermodynamic comparison with the corresponding LNAzymes (termed Lz122), using a short 17-mer RNA substrate.

The rate constant for cleavage of the 17-mer RNA within the enzyme-substrate complex (k_2) was measured in single-turnover reactions (ensuring that the product dissociation step did not affect the observed kinetics) and at saturating deoxyribozyme concentrations (≥ 1 μM; see Ref. 22). Dz122 and Lz122 showed very similar k_2 values, both at 25 and 37 °C (Table 1), indicating that the introduction of the four LNA monomers in the 8–17 arms has only marginal effects on the intramolecular strand-scission step.

The measured association rate constants (k_1) also showed differences of less than 2-fold between Dz122 and Lz122 (Table 1), in agreement with previous indications that LNAs have only minimal effects on the hybridization rate between short oligonucleotides (18). Much larger differences were observed when measuring k_{-1}, the rate constant for dissociation of the enzyme-substrate complex. The values of k_{-1} for Dz122 and Lz122 differed by more than 10-fold, reflecting the different stabilities of binding for the two catalysts. From the kinetic

constants k_1 and k_{-1}, we could also calculate the thermodynamic constant for substrate dissociation ($K_S = k_{-1}/k_1$), which was ~25-fold lower for the LNAzyme (Table 1).

These data were buttressed by UV melting studies on the complexes formed by the enzymes with a noncleavable substrate analog, bearing a single deoxyribonucleotide at the cleavage site. The experiments showed that the melting temperature (T_m) for the complex between Lz122 and the substrate analog was ≈20 °C higher than for the Dz122 complex (58 °C *versus* 38 °C, using 2 μM catalyst and 2 μM substrate analog; see supplemental Fig. 2). These findings are in agreement with published data, which report that the T_m of short DNA-RNA duplexes is increased by 4–7 °C per each pyrimidine LNA monomer introduced in the DNA sequence (30–32). The results also indicate that, with length and sequence of the binding arms being equal, an LNAzyme can be employed at a range of temperatures much wider than its all-DNA counterpart (supplemental Fig. 3).

Activities of Dz122 and Lz122 as a Function of Catalyst Concentration and Mg^{2+} Concentration—The higher thermodynamic stability of the LNAzyme-substrate complex, coupled with the minimal effects of LNA on the cleavage step, implies that LNAzymes can outperform DNAzymes under a number of conditions. For example, when measuring substrate cleavage as a function of catalyst concentration, at 37 °C, Lz122 was substantially more efficient than Dz122 at concentrations <50 nM (Fig. 3*A*). Presumably, the lower K_S value of Lz122 allowed this catalyst to saturate its substrate more easily.

We also compared the Mg^{2+} dependences of activity for Dz122 and Lz122. It is known that the intramolecular reaction rate (k_2) of 8–17 is stimulated by Mg^{2+} and that such activation follows a hyperbolic titration curve (22); also, the thermodynamic substrate dissociation constant, K_S, is expected to decrease as the concentration of Mg^{2+} increases (33). When we tested Dz122 and Lz122 (at a fixed 100 nM concentration) *versus* [Mg^{2+}], the LNAzyme activity showed a hyperbolic dependence, whereas the curve for Dz122 was sigmoidal, indicating an apparently cooperative activation (Fig. 3*B*). As a result, the LNAzyme was significantly superior to the DNAzyme at [Mg^{2+}] ≤ 1.5 mM (Fig. 3*B*). We explain these findings as follows. For Lz122, the 100 nM catalyst concentration is sufficient to saturate the substrate over the whole range of [Mg^{2+}] explored, so that only the effect on k_2 is apparent. Dz122, however, is unable to saturate its substrate at low magnesium concentrations, hence performing with suboptimal efficiency. The apparent cooperativity arises because Mg^{2+}
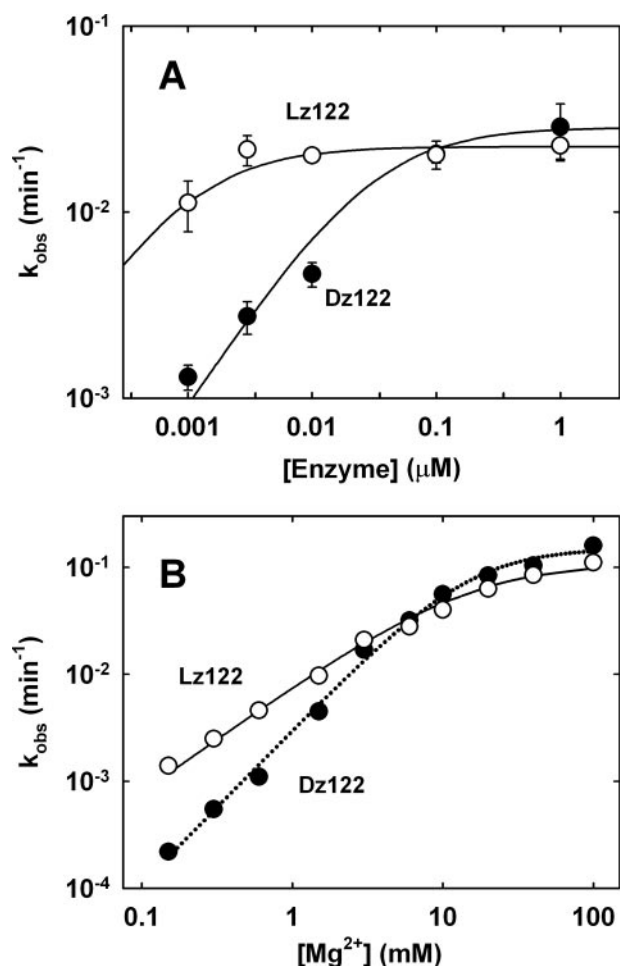
FIGURE 3. *A,* concentration dependence of the cleavage rates observed with Dz122 and Lz122 at 37 °C, pH 7.4, 3 mM Mg^{2+}. *Error bars* represent the range of variation in duplicate experiments. The data were fit to the following: $k_{obs} = (k_2 \times [E])/(K_S + [E])$, where $[E]$ represents the catalyst concentration. The *solid lines* through the data represent binding curves with K_S = 30 nM (Dz122) and 1 nM (Lz122). The estimated 30-fold greater affinity of Lz122 for its substrate compares well with the 24-fold difference obtained at 25 °C (Table 1). *B,* Mg^{2+} dependence of the cleavage rates. Conditions as in *A,* except that the concentration of the catalyst was constant (100 nM) and the concentration of Mg^{2+} varied from 0.15 to 100 mM. The *solid line* through the Lz122 data is the best fit to a binding hyperbola with K_d = 14 mM. The *dotted line* through the Dz122 data is the best fit to the Hill equation (23). The Hill coefficient, n, gauging the apparent cooperativity of Mg^{2+} activation, was 1.4.

ions, at low concentrations, stimulate both formation of the Dz122-substrate complex (effect on K_S) and catalysis within the complex (effect on k_2).

LNAzymes, but Not DNAzymes, Cleave Efficiently the Folded E6 and E6E7 Transcripts—We next compared the relative cleavage efficiencies of 8–17 DNAzymes and LNAzymes against targets that are embedded in large, structured RNA molecules. To this end, we assayed the ability of the four DNAzymes and of the respective LNAzymes to cleave the full-length E6 transcript (E6 mRNA, 544 nt long). Table 2 summarizes the results obtained with this long transcript, together with controls where minimal (19-mer) substrates were used. Note that during HPV16 infection, the E6 sequence is part of a polycistronic mRNA that also encodes the E7 oncoprotein; accordingly, as a further control, we tested the DNAzymes and LNAzymes also against an E6E7 polycistronic transcript (E6E7 mRNA 830 nt long; supplemental Fig. 1).

Reaction rates were initially measured using "protocol A" (see "Experimental Procedures"). In this protocol, mRNA transcripts are allowed to fold into stable structures (presumably similar to the structures adopted in the cytoplasm) prior to being exposed to the catalysts. Under these conditions, the LNAzymes (at a 100 nM concentration) could efficiently cleave the long RNAs (Fig. 4*A*), yielding kinetic time courses that were well described by simple exponential functions (Fig. 4*B*). The observed rate constants closely resembled those measured for the cleavage of minimal substrates (Table 2, *left*). Moreover, the rates of cleavage were virtually unchanged when the four LNAzymes were tested against the E6 mRNA or the E6E7 mRNA, despite the additional ~300 nt in the E6E7 transcript (supplemental Table 1).

Although three of four LNAzymes showed similar activities against the long RNAs, Lz51 cleaved much more slowly and to a lower extent (Fig. 4*B*). As stated above, previous studies implied that the target sequence of Lz51 could be intrinsically less accessible than those of the other three constructs, but this would not explain why Lz51 behaved poorly even against a short 19-mer substrate (Table 2). A more likely explanation lies in the propensity of free Lz51 to adopt alternative secondary structures, which are expected to reduce binding of the substrate and hence catalysis (supplemental Fig. 4). In agreement with this hypothesis, control experiments suggested that the LNAzyme, at the 100 nM concentration used, was far from saturating its E6 substrate (data not shown). Despite these problems, it is remarkable that Lz51 was able to access and cleave its target within the long RNAs, whereas the corresponding all-DNA construct, Dz51, failed to cleave at concentrations as high as 10 μM (Table 2 and data not shown).

Indeed, in strong contrast to the LNAzymes, all four of the DNAzymes showed a nearly complete inability to cleave the long substrates under the protocol A conditions (Table 2, *left*). This suggests that the local RNA structure prevents the access of unmodified 8–17 DNAzymes to fully folded targets, exacerbating the differences in activity between DNAzymes and LNAzymes.

Cleavage of the E6 mRNA Under "Pre-annealing" Conditions—Could the performance gap between DNAzymes and LNAzymes be reduced by allowing the catalysts to encounter an unfolded target? To address this possibility, we measured cleavage of the E6 transcript using a distinct protocol (protocol B), where the LNAzyme (or DNAzyme) and its substrate were mixed together, heated at 80 °C for 2 min, and cooled at 37 °C prior to starting the cleavage reaction. This protocol represents a stage between the cleavage of a fully folded mRNA and the cleavage of a minimal, unstructured substrate; the denaturation step at 80 °C is expected to disrupt the local secondary and tertiary structures, thus allowing a direct access of the catalysts to their targets, even though binding of the catalysts (during cooling) would have to compete with the refolding process of the long RNA.

For the LNAzymes the differences between the data from the two protocols were mostly minor (Table 2). On the other hand, three of the all-DNA constructs, which were essentially inactive against the pre-folded long transcripts, showed in this case an appreciable ability to cleave the E6 RNA (Table 2, *right*), albeit

TABLE 2

Performance of DNAzymes and LNAzymes against the E6 mRNA transcript

Conditions used are as follows: Tris-HCl buffer, pH 7.5, 10 mM Mg^{2+}, 37 °C. Cleavage was performed under single-turnover conditions, using 10 nM substrate and 100 nM catalyst (DNAzyme or LNAzyme). In experiments with the 19-mer substrates, the 100 nM concentration was saturating for the LNAzymes (except for Lz51) but slightly subsaturating for the DNAzymes, as the observed reaction rates of Dz32, Dz122, and Dz163 increased by 1.5–2-fold when the DNAzyme concentration was raised to 1 μM. The kinetic time courses were fit to Equation 1, where F_∞ indicates the final extent of cleavage. For each reaction, the reported k_{obs} values are the average of two to four independent experiments. k_{obs} values from individual experiments differed by no more than 20% from the mean, except for reactions of DNAzymes with the E6 RNA (protocol B conditions) where the range of variation was within ±40% of the mean.

	Protocol A (cleavage of pre-folded RNA)				Protocol B (cleavage after pre-annealing catalyst and substrate)			
	19-mer substrate		E6 mRNA		19-mer substrate		E6 mRNA	
	k_{obs}	F_∞	k_{obs}	F_∞	k_{obs}	F_∞	k_{obs}	F_∞
	min^{-1}		min^{-1}		min^{-1}		min^{-1}	
Lz32	4.6×10^{-2}	0.79	4.4×10^{-2}	0.64	6.6×10^{-2}	0.73	4.5×10^{-2}	0.67
Lz51[a]	3.6×10^{-3}	0.80	5.5×10^{-3}	0.44	2.6×10^{-3}	0.50	1st, 5.2×10^{-2}	$F_1 = 0.12$
							2nd, 2.0×10^{-3}	$F_2 = 0.64$
Lz122[b]	2.0×10^{-2}	0.68	2.5×10^{-2}	0.80	3.7×10^{-2}	0.74	4.1×10^{-2}	0.75
Lz163[c]	2.9×10^{-2}	0.85	3.2×10^{-2}	0.85	0.14	0.76	5.2×10^{-2}	0.86
Dz32[d]	1.6×10^{-2}	0.90	$\leq 10^{-4}$		2.1×10^{-2}	0.90	2.7×10^{-3}	0.15
Dz51[e]	$\leq 7 \times 10^{-5}$				$\leq 7 \times 10^{-5}$			
Dz122[f]	3.8×10^{-2}	0.80	$\leq 7 \times 10^{-5}$		5.0×10^{-2}	0.82	5.6×10^{-4}	0.30
Dz163[f]	1.3×10^{-2}	0.90	$\leq 7 \times 10^{-5}$		1.3×10^{-2}	0.90	2.7×10^{-4}	0.30

[a] When Lz51 was tested according to protocol B, the kinetics of cleavage of the long RNA substrates were distinctly biphasic. The data were therefore fit to Equation 2, and the table reports the rate constants and the extent of cleavage for both phases.

[b] To compare these data with the data in Table 1, the reaction of Lz122 (100 nM) against the E6 transcript was also tested in the presence of 3 mM Mg^{2+}, yielding $k_{obs} = 1.6 \times 10^{-2}$ min^{-1} and $F_\infty = 0.74$.

[c] Lz163 cleaved its 19-mer substrate ~4-fold faster under the protocol B conditions than with protocol A. The behavior was reproducible but remains unexplained, since the minimal substrate of Lz163 is not expected to form any stable secondary structure.

[d] When Dz32 was tested against the E6 transcript according to protocol A, less than 5% of product was formed in 10 h. During this time, some unspecific degradation of the long mRNA also began to occur. Based on these data, and assuming an end point of 0.9, we estimated that cleavage by Dz32 would occur with a $k_{obs} \leq 10^{-4}$ min^{-1}.

[e] The reaction of 100 nM Dz51 with the 19-mer substrate was too slow to be reliably measured (no appreciable product formation in 8 h). By using a 10-fold higher concentration of catalyst, we measured kinetics with an apparent end point of 0.60 and observed rate constants of 7×10^{-4} min^{-1} (with both protocols).

[f] Upper limits for the rates of E6 cleavage were estimated as in Footnote d, except that less than 4% product was formed in 10 h.

with lower rates as compared with LNAzymes and with a modest overall yield.

DISCUSSION

We have incorporated four or five LNA monomers in the arms of the 8–17 deoxyribozyme and have shown that such a modification substantially improves the deoxyribozyme performances under a number of conditions. This result parallels those reported in previous studies on the 10–23 motif (11, 13–16), demonstrating that the inclusion of LNA monomers in the target-binding arms is advantageous for deoxyribozymes in general. More fundamentally, our work has addressed the mechanistic basis of the advantages conferred by LNAs, providing a detailed rationale for the effects reported by us and by other authors.

LNAzyme Advantages in the Cleavage of Short, Unstructured Substrates—The kinetic data obtained with short RNA substrates indicate that deployment of LNA monomers in the 8–17 arms (at least, at positions not immediately adjacent to the central core) does not have major effects on the intrinsic rate of cleavage, described by k_2 in Fig. 1B. This conclusion stems from the detailed comparison between Dz122 and Lz122 (Table 1) as well as from data on the Dz32/Lz32 and Dz163/Lz163 couples (see legend of Table 2). The point is not trivial, as previous studies suggested that alterations in the helices formed by the 8–17 arms could substantially affect catalysis (34, 35).

On the other hand, the comparison between Dz122 and Lz122 confirms that LNA monomers enhance binding of the deoxyribozyme to its target, raising the thermodynamic stability of the enzyme-substrate complex in consistency with published studies on short LNA-containing duplexes (30–32). In

principle, this effect could partially arise from an improvement in hybridization kinetics, because the association rate constant (k_1) for the unmodified 8–17 is about 10-fold lower than the constants typical for the annealing of short complementary oligonucleotides (22, 36, 37). However, k_1 values for Lz122 and Dz122 were very similar, in agreement with previous indications that LNAs do not accelerate substantially the hybridization between short, unstructured oligonucleotides (18). Thus, the LNA-mediated increase in binding affinity can be attributed almost entirely to slowed down kinetics of substrate release (Table 1).[5]

The higher substrate affinity of the LNAzymes means that they can saturate their substrates and reach maximum catalytic efficiency at much lower concentrations than DNAzymes having the same sequence. For example, Fig. 3A shows that in reactions carried out at 1 nM enzyme, Lz122 is about 10-fold more efficient than Dz122 in cleaving a minimal substrate. This gap is predicted to become even wider if lower concentrations of catalyst were used; the maximum difference in k_{obs} (attainable at enzyme concentrations well below the K_S of Lz122) is predicted to be ~30-fold, directly mirroring the difference in affinity between LNAzyme and DNAzyme (Fig. 3A).

It is very likely that the 10–23 LNAzyme constructs described in previous studies (11–17) behave similar to Lz122. The lower concentration requirements may explain, for exam-

---

[5] This conclusion presumably also holds for the 10–23 constructs described in previous studies (11–16). The association rates for the 10–23 deoxyribozyme already approach those observed for short complementary oligonucleotides (k_{-1} values $>10^8$ min^{-1}) (36, 37), and it seems unlikely that these rates may be substantially increased in LNA-armed constructs.
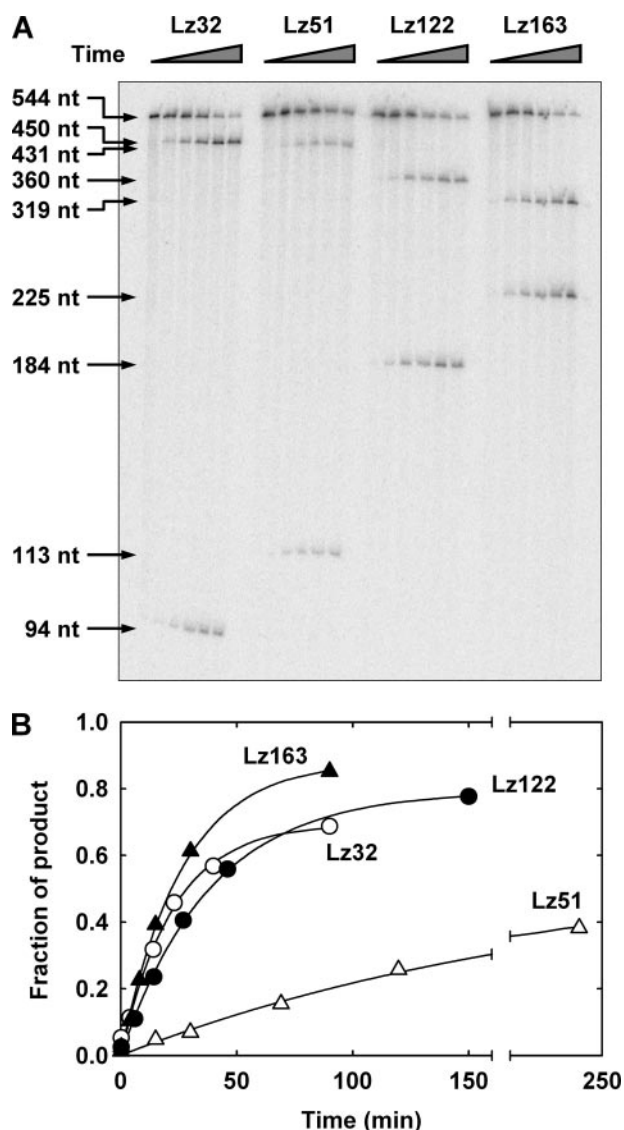
Kinetic Properties of LNA-armed Deoxyribozymes

FIGURE 4. *A,* single-turnover reaction of the LNAzymes under protocol A conditions. The internally labeled E6 transcript (544 nt long; 10 nM final concentration) reacted with each of the four LNAzymes (100 nM) at 37 °C, pH 7.5, 10 mM Mg²⁺. Aliquots were collected at appropriate times, and the substrate and products were separated on a 5% polyacrylamide denaturing gel. *B,* time courses of the cleavage reactions shown in *A.* The *solid lines* represent least squares fits of the experimental data to Equation 1.

ple, earlier data showing that the activity of 10–23 against a short RNA substrate was improved by including LNA monomers within the deoxyribozyme arms (11). In fact, those data were collected at nanomolar concentrations of catalyst, that is under conditions that presumably did not allow efficient substrate binding by the all-DNA construct but permitted a stable binding and cleavage by the LNAzyme.

LNAzyme Advantages in the Cleavage of Long Structured Substrates—In the presence of long substrates, the disparity in performance between DNAzymes and LNAzymes is impressive, and it does not seem to simply reflect the diverse binding affinities for the two types of catalysts. In particular, we just noted that the difference in activity between Dz122 and Lz122, predicted from experiments with a minimal substrate and attributable to the relative binding affinities, should be at most

~30-fold. The actual difference observed against the long transcripts, however, greatly exceeds this value (Table 2, protocol A). More fundamentally, the differences in substrate binding affinities (K_S) or in substrate dissociation rates (k_{-1}) would not explain why the performance gap between DNAzymes and LNAzymes depends on the reaction protocol, *i.e.* why cleavage of the E6 RNA by the DNAzymes (but not LNAzymes) is improved by pre-annealing the catalysts to their targets (Table 2).

When DNAzymes and LNAzymes are reacted with the fully folded E6 transcript (*i.e.* under protocol A conditions), the local RNA structure represents a kinetic barrier to binding of the catalysts, which is expected to slow down the association process; under this condition, LNAzymes performed well, whereas the activity of DNAzymes was hardly measurable. The heating and cooling step in protocol B allows a direct access of the catalysts to their target sequences, removing at least in part the initial kinetic barrier to association; in this case, Dz32, Dz122, and Dz163 showed a substantially increased activity (Table 2). Hence, our data suggest that annealing to a folded substrate is *kinetically* much more difficult for DNAzymes than for LNAzymes. Put another way, the data in Table 2 suggest that LNAzymes bind to structured targets with a faster association rate (k_{-1}) as compared with DNAzymes.

This conclusion is not completely unexpected. Previous studies on 10–23 constructs had implicitly suggested that LNA facilitates the kinetics of deoxyribozyme annealing to structured RNA (11, 14, 16). Moreover, in contrast with earlier results obtained with short, *unstructured* oligonucleotides (18), Ormond *et al.* (19) recently showed that the hybridization between *structured* oligonucleotides (*i.e.* oligonucleotides forming an intramolecular stem-loop) could be accelerated by including a few LNA residues in one of the two complementary strands.

A Model for LNAzymes Reacting with Structured Substrates— LNA did not greatly affect the kinetics of 8–17 binding to a short substrate, so why should things be different with long, folded RNAs? Binding of a DNAzyme to a structured target is almost certainly a more complex phenomenon than annealing to a minimal substrate, and it presumably occurs through the formation of intermediates in which the hybridization is only partially complete (38, 39). For example, a simple two-step model can be envisaged, whereby the enzyme initially base pairs to a stretch of just a few accessible residues (nucleation), after which the hybridization proceeds to completion, leading to disruption of the local RNA secondary structure (Fig. 5).

Analogous models have been suggested before in other systems. For example, while this paper was in preparation, a model very similar to the one in Fig. 5 was proposed to explain the binding of micro-RNAs to their target sequences within structured mRNAs; the model was also shown to account accurately for a series of *in vivo* results (40). Micro-RNAs and deoxyribozymes are both short oligonucleotides with an extended, but not perfect, complementarity to their targets; thus it seems reasonable that their binding mechanisms may share several common features.

The two-step model offers an explanation as to why LNAzymes can bind faster than DNAzymes to structured tar-
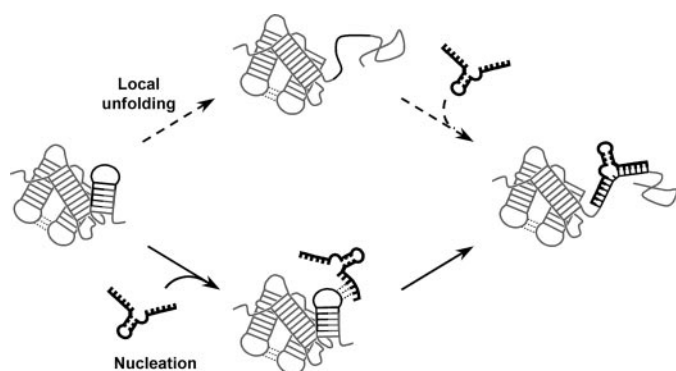
FIGURE 5. **A schematic model for the binding of DNAzymes and LNAzymes to target sequences embedded in large structured RNAs.** In principle, the catalyst may bind to its target when the target sequence becomes completely accessible, thanks to a local unfolding event (*e.g.* the occasional fraying of a double helix; upper pathway). Binding to a fully accessible target, however, is presumably very rare in the context of a large mRNA, at physiological temperatures. More often, complete hybridization of the catalyst may entail formation of binding intermediates, which precede and favor the disruption of the local mRNA structure. For example, the enzyme might initially form interactions with a few unpaired nucleotides on the target (*Nucleation*; lower pathway). Such interactions would be particularly stable for LNA-armed catalysts, thereby promoting a more efficient disruption of the local structure and a faster completion of binding. Note that other types of intermediates (*e.g.* triple-stranded species) might be formed during the initial nucleation events: whatever the nature of these transient intermediates, their stabilization might ease the overall binding process.

gets. In fact, normal DNAzymes would form relatively weak interactions in the initial nucleation complex, so that the catalyst would generally fall off before completing the hybridization process. For the LNAzymes, however, nucleation would yield a more stable binding intermediate, providing a bridgehead for the invasion of the nearby structure and therefore promoting a faster formation of the catalyst-substrate complex. Once formed, this complex would be more stable than the corresponding DNAzyme-substrate complex (because of the intrinsically lower k_{-1}), thus reducing the chances that the catalyst may dissociate before cleaving.

Although the model in Fig. 5 certainly needs to be further refined and tested, it represents a useful starting point for future mechanistic analyses. The model has implications not just for LNAzymes but also, more generally, for oligonucleotides containing residues that form especially strong base pairs with RNA, be they LNA, 2'-*O*-methyl nucleotides, or other monomers. The model predicts that, broadly speaking, these modified oligonucleotides will bind to structured RNA at a faster rate as compared with unmodified oligonucleotides. The actual extent of acceleration would presumably depend on factors such as the number and location of the modified monomers within the oligonucleotide.

Multiple Turnover and Specificity Issues—The data obtained in this work demonstrate the advantages of introducing LNA monomers in the deoxyribozyme arms. In principle, however, the use of LNAzymes may be disadvantageous under some conditions.

In particular, LNA-armed deoxyribozymes are expected to interact strongly with the cleavage products, a feature that may decrease the reaction rate under multiple turnover conditions. This problem, however, should arise only when the deoxyribozyme arms contain a high number of LNA monomers.

Indeed, recent studies have shown that LNAzymes containing just two LNA monomers on each arm (similar to Dz122) function usually better than plain DNAzymes under multiple-turnover conditions (16, 17).

The possibility of off-target binding is also an important concern. In fact, LNA monomers could favor annealing of a deoxyribozyme not only to the intended target but also to sequences that differ from the target by just a few nucleotides. Nevertheless, data in the literature suggest that mismatches involving LNA monomers are not more stable than normal mismatches (41) and that, in general, LNA improves the single-nucleotide mismatch discrimination with respect to that obtained with DNA (41, 42). We also note that the LNAzymes used in this study showed no sign of off-target cleavage within the E6 mRNA (Fig. 4*A*) or the E6E7 mRNA (not shown).

CONCLUSIONS

We have analyzed in detail the kinetic and thermodynamic properties of LNA-containing deoxyribozymes, highlighting the mechanistic differences between these catalysts and their all-DNA counterparts. Overall, the results of this work emphasize that the advantageous features of LNAzymes become fully manifest when performing reactions at low catalyst concentrations, at low magnesium concentrations, and against large structured RNAs. These are exactly the conditions that are expected to occur in cells, helping to explain why LNA-armed deoxyribozymes have proven substantially superior to conventional DNAzymes for the knockdown of specific mRNAs *in vivo* (13, 17).

REFERENCES

1. Silverman, S. K. (2005) *Nucleic Acids Res.* **33,** 6151–6163
2. Santoro, S. W., and Joyce, G. F. (1997) *Proc. Natl. Acad. Sci. U. S. A.* **94,** 4262–4266
3. Cairns, M. J., Saravolac, E. G., and Sun, L. Q. (2002) *Curr. Drug Targets* **3,** 269–279
4. Dass, C. R. (2004) *Trends Pharmacol. Sci.* **25,** 395–397
5. Dass, C. R. (2006) *Drug. Dev. Ind. Pharm.* **32,** 1–5
6. Cairns, M. J., Hopkins, T. M., Witherington, C., Wang, L., and Sun, L. Q. (1999) *Nat. Biotechnol.* **17,** 480–486
7. Kurreck, J., Bieber, B., Jahnel, R., and Erdmann, V. A. (2002) *J. Biol. Chem.* **277,** 7099–7107
8. Vester, B., and Wengel, J. (2004) *Biochemistry* **43,** 13233–13241
9. McTigue, P. M., Peterson, R. J., and Kahn, J. D. (2004) *Biochemistry* **43,** 5388–5405
10. Kaur, H., Arora, A., Wengel, J., and Maiti, S. (2006) *Biochemistry* **45,** 7347–7355
11. Vester, B., Lundberg, L. B., Sorensen, M. D., Babu, B. R., Douthwaite, S., and Wengel, J. (2002) *J. Am. Chem. Soc.* **124,** 13682–13683
12. Schubert, S., Gul, D. C., Grunert, H. P., Zeichhardt, H., Erdmann, V. A., and Kurreck, J. (2003) *Nucleic Acids Res.* **31,** 5982–5992
13. Fahmy, R. G., and Khachigian, L. M. (2004) *Nucleic Acids Res.* **32,** 2281–2285
14. Schubert, S., Furste, J. P., Werk, D., Grunert, H. P., Zeichhardt, H., Erdmann, V. A., and Kurreck, J. (2004) *J. Mol. Biol.* **339,** 355–363

15. Fluiter, K., Frieden, M., Vreijling, J., Koch, T., and Baas, F. (2005) *Oligonucleotides* **15,** 246–254

16. Vester, B., Hansen, L. H., Lundberg, L. B., Babu, R., Sorensen, M. D., Wengel, J., and Douthwaite, S. (2006) *BMC Mol. Biol.* **7,** 19

17. Jakobsen, M. R., Haasnoot, J., Wengel, J., Berkhout, B., and Kjems, J. (2007) *Retrovirology* **4,** 29

18. Christensen, U., Jacobsen, N., Rajwanshi, V. K., Wengel, J., and Koch, T. (2001) *Biochem. J.* **354,** 481–484

19. Ormond, T. K., Spear, D., Stoll, J., Mackey, M. A., and St. John, P. M. (2006) *J. Biomol. Struct. Dyn.* **24,** 171–182

20. Wengel, J. P. (1999) *Acc. Chem. Res.* **32,** 301–310

21. Cantor, C. R., Warshaw, M. M., and Shapiro, H. (1970) *Biopolymers* **9,** 1059–1077

22. Bonaccio, M., Credali, A., and Peracchi, A. (2004) *Nucleic Acids Res.* **32,** 916–925

23. Fersht, A. R. (1985) *Enzyme Structure and Mechanism*, pp. 137–273, W. H. Freeman & Co., New York

24. Venturini, F., Braspenning, J., Homann, M., Gissmann, L., and Sczakiel, G. (1999) *Nucleic Acids Res.* **27,** 1585–1592

25. Pan, W. H., Xin, P., Bui, V., and Clawson, G. A. (2003) *Mol. Ther.* **7,** 129–139

26. Cairns, M. J., and Sun, L. Q. (2004) *Methods Mol. Biol.* **252,** 267–277

27. Zuker, M. (2003) *Nucleic Acids Res.* **31,** 3406–3415

28. Peracchi, A., Bonaccio, M., and Clerici, M. (2005) *J. Mol. Biol.* **352,** 783–794

29. Ferrari, D., and Peracchi, A. (2002) *Nucleic Acids Res.* **30,** e112

30. Singh, S. K., Nielsen, P., Koshkin, A. A., and Wengel, J. (1998) *Chem. Commun.* 455–456

31. Singh, S. K., and Wengel, J. (1998) *Chem. Commun.* 1247–1248

32. Bondensgaard, K., Petersen, M., Singh, S. K., Rajwanshi, V. K., Kumar, R., Wengel, J., and Jacobsen, J. P. (2000) *Chemistry* **6,** 2687–2695

33. Nakano, S., Fujimoto, M., Hara, H., and Sugimoto, N. (1999) *Nucleic Acids Res.* **27,** 2957–2965

34. Li, J., Zheng, W., Kwon, A. H., and Lu, Y. (2000) *Nucleic Acids Res.* **28,** 481–488

35. Liu, Y., and Sen, D. (2004) *J. Mol. Biol.* **341,** 887–892

36. Santoro, S. W., and Joyce, G. F. (1998) *Biochemistry* **37,** 13330–13342

37. Joyce, G. F. (2001) *Methods Enzymol.* **341,** 503–517

38. Reynaldo, L. P., Vologodskii, A. V., Neri, B. P., and Lyamichev, V. I. (2000) *J. Mol. Biol.* **297,** 511–520

39. Walton, S. P., Stephanopoulos, G. N., Yarmush, M. L., and Roth, C. M. (2002) *Biophys. J.* **82,** 366–377

40. Long, D., Lee, R., Williams, P., Chan, C. Y., Ambros, V., and Ding, Y. (2007) *Nat. Struct. Mol. Biol.* **14,** 287–294

41. You, Y., Moreira, B. G., Behlke, M. A., and Owczarzy, R. (2006) *Nucleic Acids Res.* **34,** e60

42. Mouritzen, P., Nielsen, A. T., Pfundheller, H. M., Choleva, Y., Kongsbak, L., and Moller, S. (2003) *Expert Rev. Mol. Diagn.* **3,** 27–38

The Advantages of Being Locked: ASSESSING THE CLEAVAGE OF SHORT AND LONG RNAs BY LOCKED NUCLEIC ACID-CONTAINING 8–17 DEOXYRIBOZYMES

Stefano Donini, Marcello Clerici, Jesper Wengel, Birte Vester and Alessio Peracchi